Assessing the chronic effect of the bioavailable fractions of radionuclides and heavy metals on stream microbial communities: A case study at the Rophin mining site

Clarisse Mallet, Florent Rossi, Yahaya Hassan-Loni, Guillaume Holub, Le Thi-Hong-Hanh, Olivier Diez, Hervé Michel, Claire Sergeant, Sofia Kolovi, Patrick Chardon, et al.

Science of the Total Environment 919 (2024) 170692

Contents lists available at ScienceDirect

Science of the Total Environment

journal homepage: www.elsevier.com/locate/scitotenv

Assessing the chronic effect of the bioavailable fractions of radionuclides and heavy metals on stream microbial communities: A case study at the Rophin mining site

Clarisse Mallet [a,i,*], Florent Rossi [g,h], Yahaya Hassan-Loni [b], Guillaume Holub [c,i], Le Thi-Hong-Hanh [e,i], Olivier Diez [d,i], Hervé Michel [e,i], Claire Sergeant [c,i], Sofia Kolovi [f,i], Patrick Chardon [f,i], Gilles Montavon [b,i,**]

[a] Université Clermont-Auvergne, CNRS, Laboratoire Microorganismes: Génome et Environnement, F-63170 Aubière, France
[b] SUBATECH, IMT Atlantique, Nantes Université, CNRS, F-44000 Nantes, France
[c] Univ. Bordeaux, CNRS, LP2I Bordeaux, UMR5797, F- 33170 Gradignan, France
[d] Institut de Radioprotection et Sureté Nucléaire (IRSN), PSE-ENV/SPDR/LT2S, 31 Avenue de la division Leclerc, F-922602 Fontenay-aux-Roses, France
[e] ICN UMR 7272, Université Côte d'Azur, 28 avenue Valrose, 06108 Nice, France
[f] Université Clermont-Auvergne, CNRS, LPC Clermont, F-63170 Aubière, France
[g] Département de biochimie, de microbiologie et de bio-informatique, Faculté des sciences et de génie, Université Laval, Québec, Canada
[h] Centre de recherche de l'institut de cardiologie et de pneumologie de Québec, Québec, Canada
[i] LTSER "Zone Atelier Territoires Uranifères", F-63170, France

HIGHLIGHTS

- Available fractions of uranium and radium were high and varied from sites.
- Bacterial and fungal compositions were impacted by the contaminants.
- Fungal diversity was higher in the most contaminated site compared to the reference.
- Bacterial functions related to nitrogen and carbon impaired in contaminated sites.

GRAPHICAL ABSTRACT

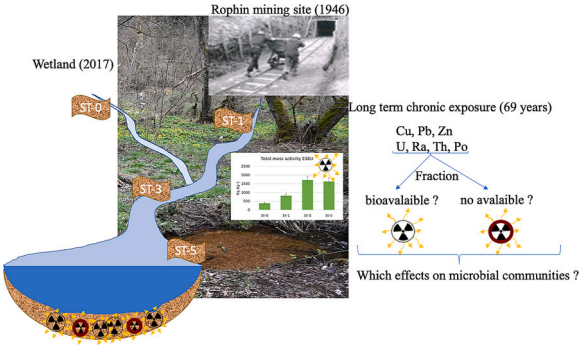

ARTICLE INFO

Editor: Jay Gan

Keywords:
Bioavailability
Radionuclides
Heavy metals

ABSTRACT

This study aimed to assess the potential impact of long-term chronic exposure (69 years) to naturally-occurring radionuclides (RNs) and heavy metals on microbial communities in sediment from a stream flowing through a watershed impacted by an ancient mining site (Rophin, France). Four sediment samples were collected along a radioactivity gradient (for ^{238}U368 to 1710 Bq.Kg^{-1}) characterized for the presence of the bioavailable fractions of radionuclides (^{226}Ra, ^{210}Po), and trace metal elements (Th, U, As, Pb, Cu, Zn, Fe).

* Correspondence to: C. Mallet, Université Clermont-Auvergne, CNRS, Laboratoire Microorganismes: Génome et Environnement, F-63170, Aubière, France.
** Correspondence to: G. Montavon, SUBATECH, IMT Atlantique, Nantes Université, CNRS, SUBATECH, F-44000 Nantes, France.
E-mail addresses: clarisse.mallet@uca.fr (C. Mallet), montavon@subatech.in2p3.fr (G. Montavon).

https://doi.org/10.1016/j.scitotenv.2024.170692
Received 18 October 2023; Received in revised form 8 January 2024; Accepted 2 February 2024
Available online 5 February 2024

Microbial community
bacteria
fungi

Results revealed that the available fraction of contaminants was significant although it varied considerably from one element to another (0 % for As and Th, 5–59 % for U). Nonetheless, microbial communities appeared significantly affected by such chronic exposure to (radio)toxicities. Several microbial functions carried by bacteria and related with carbon and nitrogen cycling have been impaired. The high values of fungal diversity and richness observed with increasing downstream contamination ($H' = 4.4$ and Chao1 = 863) suggest that the community had likely shifted toward a more adapted/tolerant one as evidenced, for example, by the presence of the species *Thelephora* sp. and *Tomentella* sp. The bacterial composition was also affected by the contaminants with enrichment in *Myxococcales, Acidovorax* or *Nostocales* at the most contaminated points.

Changes in microbial composition and functional structure were directly related to radionuclide and heavy metal contaminations, but also to organic matter which also significantly affected, directly or indirectly, bacterial and fungal compositions. Although it was not possible to distinguish the specific effects of RNs from heavy metals on microbial communities, it is essential to continue studies considering the available fraction of elements, which is the only one able to interact with microorganisms.

1. Introduction

Over the last 60 years, anthropogenic activities related to the demand for nuclear energy have led to the development of 4300 uranium mines globally (Abdelouas, 2006; Dang et al., 2018). Subsequently, billions of cubic meters of tailings contaminated with multiple toxic elements like heavy metals and radionuclides (RNs) (particularly ^{238}U, ^{226}Ra, ^{210}Po and ^{232}Th) have been exposed to the surface (Bernhard et al., 1998). Even after mining operations ceased, uranium tailings may significantly impact the surrounding environment and related biosphere for long periods (Momčilović et al., 2013; Yan and Luo, 2015). Despite effluent treatment and remediation strategies, downstream accumulation of RNs and heavy metals on natural wetland, shorelines, lake or stream sediments has been observed, further exuberating its ecotoxicological risk (Markich, 2002; Sitte et al., 2015; Stetten et al., 2018). The impact of uranium releases into the environment (and related decay products) is determined by RNs speciation, which influences their solubility, transport, bioavailability and toxicity (Abdelouas, 2006; Khemiri et al., 2014; Markich, 2002; Suriya et al., 2017). Consequently, site-specific physical and chemical features (i.e. organic or inorganic ligands as carbonates, phosphates, iron/manganese oxides, organic matters or microbial cells, etc.) likely influence the speciation and mobility of RNs, affecting their bioavailability and toxicity (Cumberland et al., 2016; Dang et al., 2018; Gadd and Fomina, 2011; Husson et al., 2019). It is therefore important to take all these factors into account when studying microbial interactions with RNs (Rogiers et al., 2021).

However, only a limited number of studies have examined the effects of RNs with or without metals on microorganisms from soil or sediment, and the existing studies are primarily focused on uranium (Detail is described in Fig. S1). Although a number of them have shown deleterious impacts of increasing concentrations of uranium on the structure of microbial communities (Hoyos-Hernandez et al., 2019; Jaswal et al., 2019; Li et al., 2018), the response of indigenous microbial communities to metal and uranium exposure is not clear (Rogiers et al., 2021). Such heterogeneity of results could be due to i) difference in U chemical and/or radiation exposures and its related effects on microorganisms (Hoyos-Hernandez et al., 2019; Jaswal et al., 2019; Mondani et al., 2011; Radeva et al., 2013) and/or ii) to the different physical and chemical properties of soils and sediments, affecting microbial communities directly and/or indirectly through changes in U bioavailability (Boteva et al., 2016; Li et al., 2018; Sitte et al., 2015). Moreover, microbial tolerance to uranium and heavy metals may arise from mechanisms of interactions with metals and radioelements, in turn affecting their speciation andmobility (Merroun and Selenska-Pobell, 2008). This process is considered more impactful toward living organisms (Chandwadkar et al., 2018). Therefore, impact studies should not rely solely on the total amount of element under consideration (Violante et al., 2010). Although the bioavailable portion of the radionuclides, related to the chemical speciation (Bresson et al., 2011; Salbu, 2007), would be more appropriate in this context, few studies assessed it (Islam and Sar, 2011; Sitte et al., 2015) (Detail is provides in Fig. S1).

Consequently, assessing the effects of naturally-occurring RNs contamination on microorganisms requires a complete knowledge of the system (composition, presence of other contaminants, etc.) as well as the potentially bioavailable fractions of contaminants (including RNs). To our knowledge, such a work has never been carried out *in natura* for microorganisms present in sediments. The aim of this project is therefore to fill this gap, using the Rophin site as the study site.

The Rophin mining site, located in the Puy-de-Dôme department (central France), has been exploited for uranium extractions from 1948 to 1954. The mining residues are today stored on an ICPE site (Installations Classified as Environmental Protection). The site is also characterized by a contaminated wetland located just downstream of the ICPE site. Several studies (Grangeon et al., 2023; Martin et al., 2020, 2021) were carried out to assess the origin of the contaminated wetland (natural vs anthropogenic) (radiation level > 1000 nSv.h^{-1}, the mean value of the local geographical background was 210 nSv.h^{-1}) (Fig. 1) and have shown that the high concentration of U present in a sediment-type layer located at around 10 cm in depth from the surface (~2000 mg.kg^{-1}) has been attributed to malfunctioning and poor maintenance of the tailings ponds resulting in a release of uranium mineral particles transported by the water. In addition to this contaminated inherited layer, the humus surface of the soil is also heavily contaminated with RNs, which would indicate a continuous input of U from the "Le Gourjeat" stream that runs through the wetland. However, many questions remain concerning the transport mode, migration behavior, bioavailability and impact of radionuclides exposure in this downstream area of the former mine site on microbial biodiversity and community structure. These are the issues addressed in the Zone Atelier Territoires Uranifères (ZATU, CNRS) research program created in 2015.

In this work, the long-term chronic effect (69 years) of the bioavailable fractions of radionuclides (^{238}U, ^{226}Ra, ^{210}Po, …) and associated heavy metals from the Rophin mining site, were assessed on microbial communities from the "Le Gourjeat" steam sediments. Additionally, the external radiotoxic effects due to uranium decay products were also considered.

To enable the conduct of this study, four sediment samples were collected along an increasing gradient of RN and heavy metal contents. In addition to considering their bioavailable fractions, a thorough characterization of the environment was conducted, including measurements of physicochemical parameters and sediment composition. As for the microbial community, richness, diversity and community structure of bacterial and fungal communities were investigated.

2. Material and methods

2.1. Study site and sampling

The Rophin mining site is located in the north-eastern part of the

Puy-de-Dome department, close to Lachaux city. It is one of 17 storage sites of uranium mining residues produced in France during the 20th century (IRSN, 2018). Today, a forest vegetation covers mine tailings and periodic water effluents from the underground galleries are collected in a trench that join the "Le Gourjeat" stream running in the watershed and a wetland downstream of the storage area (Martin et al., 2020). Further details regarding the mining site can be found in Grangeon et al. (2023) and Martin et al. (2020). The gamma dose rate results show a contamination from upstream to downstream of the watershed (Fig. 1). Accordingly, three different radiological zones of interest were defined as follow: the geological bottom (<200 $nSv.h^{-1}$), a stream downstream of the mine site (between 200 and 800 $nSv.h^{-1}$), and a radiologically marked wetland (>1000 $nSv.h^{-1}$) (Grangeon et al., 2023).

Based on the above characterization and related study, four distinct water and sediment sampling sites were selected along an upstream to downstream gradient (Fig. 1). These sites, characterized by contrasting contamination levels, included: St-1, near the storage site where radionuclides release is limited, St-3 and St-5 in the wetland area, with medium and high levels of radioactive activity respectively, indicative of potential contamination transfer to the crossing stream; and St-0 displaying the natural radioactivity circulation in this uranium-rich region (reference site).

The sampling was conducted in April 2017, and six cores of the top 2 cm of sediment were collected from each sampling site. Five of them were sampled using sterile syringes adapted to form corer (V = 0.02 L), pooled and homogenized before taking composite samples in triplicate for each biological and in duplicate for chemical analysis. They were then transported in a cooler to the laboratory and stored at −20 °C until subsequent analysis. The other core for sequential extraction of radioelements was taken with a syringe previously cleaned with a 5 % nitric acid solution and transported to the laboratory in liquid nitrogen. The water was sampled in triplicate, filtered (on 0.22 μm pore size cellulose filter) and acidified (pH ~ 1–2) before being transferred to the laboratory for chemical analysis.

Measurements of physical and chemical parameters of the stream water (conductivity, dissolved O_2, pH and alkalinity) were carried out in-situ using a CyberScan PCD 650 multi-parameter instrument and CyberScan pH 110 m (Eutech Instruments) coupled to dedicated probes and alkalinity, as HCO_3^- using a titration kit (Hach).

2.2. Chemicals and radiological analysis

All chemicals used were of analytical grade or better. ^{209}Po was provided by Eckert & Ziegler.

2.2.1. Water samples

Anions (Cl^-, SO_4^{2-}) and cations (Na^+, K^+, Ca^{2+}, Mg^{2+}) were quantified by ionic chromatography (Dionex inc. and Metrohm inc.). Trace metals (U, Cu, Th, Pb, As and Zn) were quantified by Inducted Coupled Plasma-Mass Spectrometry (ICP XSERIES 2, ThermoFisher Scientific inc.). Si and Fe were quantified in collision chamber mode (addition of H/He). Samples were diluted in a 2 % HNO_3 solution when needed.

2.2.2. Sediment samples

2.2.2.1. Chemical and radiological measurements. Some classical chemical analyses (organic matter (OM) and nitrogen and carbon total (CT,

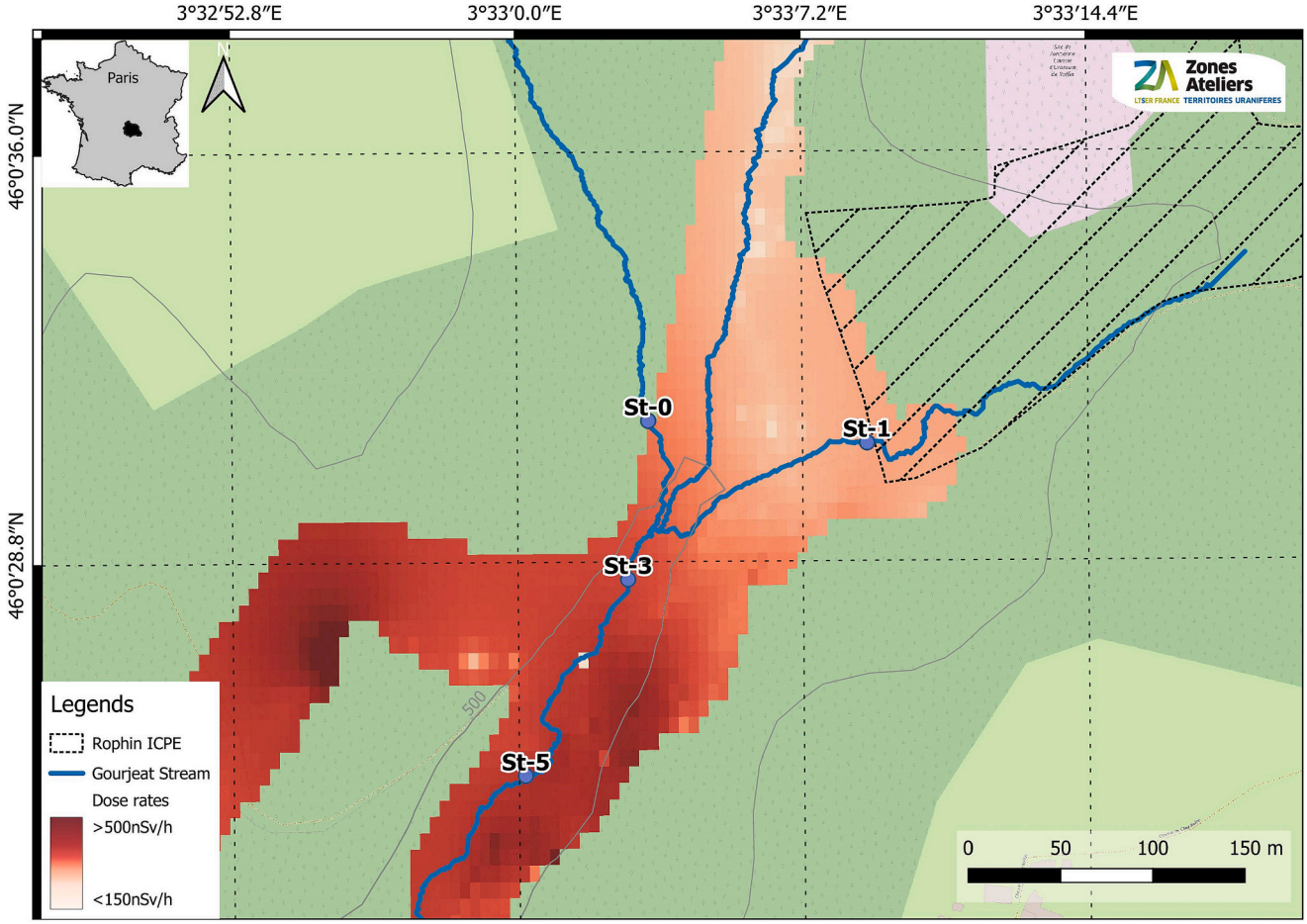

Fig. 1. Map of the study site with interpolated gamma dose rates and sampling locations.

NT) content) have been subcontracted by the company Inovalys (COFRAC (COmité FRançais d'ACcreditation) agreement numbers 1–5752, 1–5753, 1–5754, 1–5755, 1–8805).

2.2.2.1.1. Gamma-ray spectrometry. The technique allows for the identification and quantification of radionuclides based on their gamma-ray emission peaks. Sample treatment and analysis were performed under system quality insurance with the approval of French nuclear regulation authority (ASN). Samples of about 800 g of stream sediment were dried in an oven at 105 °C for 3 days. The samples were subsequently sieved to remove gravels >2 mm, crushed and sieved again at 200 μm. Approximately 60–90 g of material was then packed in a hermetically sealed Petri dish (72 × 15 mm). Gamma-ray spectrometry analysis started 30 days after preparation in order to obtain the secular equilibrium with the descendants of ^{226}Ra. Gamma ray spectrometry measurements were performed with a low-background High-Purity Germanium (HPGe) detector ("broad energy" model, ORTEC) located in a semi-underground laboratory (LP2I Bordeaux PRISNA-Platform). The spectrometer was calibrated with different Standard Reference Materials according to the NF-EN-ISO-18589-3 norm (COFRAC accreditation).

2.2.2.1.2. ^{210}Po in the sediments. Determination of total ^{210}Po activity in the sediments was done according to Le et al. (2019). Polonium activities were measured by means of alpha-spectrometry using dual alpha-spectrometers EG&G Ortec 576 A equipped with boron-implanted silicon detectors offering a 450 mm^2 active area and an alpha-resolution (FWHM) of 20 keV at 5.47 keV. Pulses were analyzed with a multichannel buffer analyzer (Spectrum Master Ortec 919) and spectra with the Vision software. The average efficiency of the detector was 22 ± 2 %. The lower limit of detection for the method employed was 0.2 mBq. Duplicate samples were prepared to ensure the quality of the analysis performed.

2.2.2.1.3. Trace elements. The content of trace metals in the sediment was determined by ICP-MS (ICP XSERIES 2, ThermoFisher Scientific inc.) after digestion following the same chemical preparation as that described in Le et al. (2019).

2.2.2.1.4. X-ray diffraction. The measurements were carried out by BRGM using the methodologies published in Grangeon et al., 2023.

2.2.2.1.5. Sequential extraction procedure. The procedure (Le et al., 2019) consists in the separation of six fractions, each starting with 0.5 g of dry sediment and introduced into centrifuge cones (50 mL): the "water soluble" fraction 1 (contact with 20 mL of demineralized water for 24 h), the exchangeable fraction 2 (residue in contact with 20 mL of 1 M NH_4OAc for 24 h), the fraction "bound-to-carbonates" 3 (residue in contact with 20 mL of buffered NaOAc/HOAc solution at pH 5.2 for 6 h), the fraction "bound-to-iron and manganese oxides" 4 (residue in contact with 20 mL of 0.04 M $NH_2OH.HCl$ for 24 h), the fraction "bound-to-organic matter" 5 (residue in contact with 15 mL of 30 % H_2O_2 acidified to pH 2 by 0.02 M HNO_3 for 24 h), and finally the "residual" fraction 6 (residue from fraction 5 transferred to a Teflon tube and mineralized by the same procedure to that previously described in Le et al., 2019). For the five first steps, suspensions are stirred at room temperature and the separation is done by centrifugation (Sigma™ 10,223) at 2000 G for 20 min. The supernatant was removed and filtered through a 0.45-μm pore size cellulose filter and analyzed by ICP-MS (U, Cu, Th, As, Zn and Pb), by emanation and scintillation counting of ^{222}Rn for ^{226}Ra (analysis realized by ALGADE), and by alpha-spectrometry for ^{210}Po (see previous section). For sensitivity reasons, only the residual fraction was analyzed for ^{226}Ra. Knowing the total quantity determined by gamma-spectrometry, it is possible by difference to determine the quantity in the first five fractions.

2.2.2.2. Assessment of radioecological risk. As mentioned in the introduction, assessing the effects is a real challenge. Given the multitude of parameters to be considered, simplifications have to be made. In order to select the most relevant RNs measured to study, the contribution of each of them to the dose rates received by microorganisms has been evaluated using ERICA tool (version 1.2). ERICA is an open-source radioecological tool which offers dose rate (μGy/h) and risk assessments in 3 levels (tiers) of incremental complexity (Brown et al., 2008) (https://erica-tool.com). Based on ICRP (International Commission on Radiological Protection) dosimetric calculation approach, ERICA employs databases of radiological factors and radiation effects (FREDERICA database) for a great variety of RNs and model organisms from freshwater (water surface, water, sediment surface, sediments), marine and terrestrial environments. The databases include among others, distribution coefficients (Kd), equilibrium Concentration Ratios (CR) and Dose Conversion Coefficients (DCC) which are essential for dose rate calculations. The suggested model organisms range from mammals and fish to insects and plants with the smallest available one, being the phytoplankton. As bacteria and fungi are not included in the tool, phytoplankton was selected as it represents the smallest organism available in ERICA. Tier assessment 2 for phytoplankton living in the sediments of a freshwater aquatic ecosystem was chosen for the current evaluation. The assessment was performed for 1 Bq.kg^{-1} of each radionuclide measured in the sediments in order to identify the higher contributor to dose rate.

2.3. Microbial communities' analyses

2.3.1. Cells extraction for estimation of prokaryote community size

Prokaryotes cells were extracted following a protocol described in Manini and Danovaro (2006) with some modifications. Following thawing at room temperature, sediment aliquots were diluted with a tetrasodium pyrophosphate solution (final concentration, 10 mM) and shaked for 30 min at 300 rpm on a rotating plate (BT300 Benckmark®). Two steps of sonication (60 s, frequency: 50 %, power: 80 W, Sonoplus Bandelin®) were carried out interrupted by vortex agitations. Supernatants were collected by centrifugation (1 min at 800 G), fixed in glutaraldehyde (1 % final concentration) and stored at 4 °C. Prokaryote counts were performed within 48 h following extraction using a BD FACSCalibur™ flow cytometer (Becton Dickinson, USA) equipped with an air-cooled laser providing 15 mW at 488 nm with the standard filter set-up. The followed procedure was described in details in Duhamel and Jacquet (2006). Briefly, extracted samples were diluted with filtered TE buffer (10 mM Tris-HCL and 1 mM EDTA, pH 8) and stained with SYBR Green 1 (10,000-fold dilution of commercial stock, Molecular Probes, Oregon, USA). Mixture was incubated for 15 min in the dark and at room temperature (~20 °C) prior to analysis. FCM list modes were analyses using CellQuest Pro software (BD Bioscences, version 4.0).

2.3.2. DNA extracting and sequencing

The composition and diversity of the microbial communities (bacteria, fungi) were analyzed from DNA extracts of approximately 0.5 g subsamples of thawed sediment (Macherey-Nagel NucleoSpin® Soil, GmbH & Co.KG, Germany), according to the manufacturer's instructions. The amount of DNA was quantified (NanoDrop technologies, Delaware USA) and adjusted to 10 ng.μL^{-1}. Aliquots were used as template to amplify the V4-V5 region of the bacteria 16 s rRNA gene with 515f (5′- GTGYCAGCMGCCGCGGTA −3′) and 928r (5′- CCCCGYCAATTCMTTTRAGT −3′) primers (Wang and Qian, 2009), and the fungi Internal Transcribed Spacer 2 (ITS2) region of the ribosomal RNA gene cluster (Ihrmark et al., 2012; Tedersoo et al., 2014) with fITS7 (5'-GTGARTCATCGAATCTTTG-3′, Ihrmark et al., 2012) and rITS4 (5'-TCCTCCGCTTATTGATATGC-3′, (White et al., 1990). All primers are supplemented with overhang adapter at the 5′ end of each primer. A PCR (Polymerase Chain Reaction) was performed in 50 μL reaction volume with the following concentrations: DNA 30 ng, 300 μM dNTPs, 0.4 μM of each both primers, 1× Kapa Hifi HotStart ReadyMix containing 2.5 mM $MgCl_2$ and 0.5 unit of Kapa Hifi HotStart® DNA polymerase (KapaBiosystems, USA). PCR cycling parameters were: 95 °C for 3 min, followed by 30 cycles at 98 °C for 20 s, 65 °C for 40 s and 72 °C for 30 s with a final extension step at 72 °C for 5 min for bacteria. For fungi, these were: 95 °C for 3 min, followed by 32 cycles at 98 °C for 20 s, 57 °C for 30 s and

72 °C for 30 s with a final extension at 72 °C for 5 min. PCR products were checked on 1 % agarose gel and quantified using the Qubit fluorimeter with Qubit® dsDNA HS reagent Assay kit (Life Technologies) before they were sent to the GeT-PLaGe plateform (INRA, Toulouse, France) for multiplexing, purification and sequencing on the Illumina MiSeq plateform.

Bacterial and fungal sequencing data were analyzed through the Frogs pipeline (respectively (Bernard et al., 2021; Escudié et al., 2018) on the Galaxy platform (Blankenberg et al., 2010; Giardine et al., 2005; Goecks et al., 2010). Briefly, sequence reads were assembled with Vsearch, and clustered into OTUs using Swarm (Mahé et al., 2014). OTU sequences were compared against the SILVA_132_16s and Unite_Fungi_8.2_20200204 databases respectively for bacteria and fungi.

Diversity indices were calculated on samples using the "*phyloseq*" package. Sample observed richness, Chao 1 index, Shannon index and Simpson's index were used to compare the sediment bacterial and fungal community α-diversities. All the statistical analyses were performed using R software (v.4.1.3).

2.3.3. Community level physiological profiles

Average Well Color Development (AWCD) and Community Level Physiological Profile (CLPP) were analyzed using Biolog EcoPlates™, containing 31 different carbon sources in three replicates (Biolog Inc., Hayward, CA, USA) (Garland and Mills, 1991). The plates' wells were inoculated with 130 µl of a bacterial cell suspension diluted 500-fold in Ringer's solution (Scharlau S.L). The size of the inoculates were adjusted to the recommended values ($> 10^6$ cell. mL^{-1}, Garland et al., 2001) based on prokaryotes abundances previously determined in all samples. The plates were incubated at 21 °C in the dark for 13 days, and plate reads (596 nm) were performed every day for 6 days with a final one at day 13 using a microplate Reader LKB 5060–006 and software package DV990 "Win 6". The raw absorbance data were corrected by subtracting the absorbance of a control sample (water) processed in the same conditions to eliminate background color from the sediment suspension. The color development of each plate was expressed as AWCD as suggested by Kenarova et al. (2014). Negative values and absorbance values <0.05 were set to zero. CLPP data analysis was elaborated as described in details in Goberna et al. (2005). The rates ($r.d^{-1}$) of color development were used to classify the microbial communities.

2.4. Statistical analyses

Statistical differences between sampling sites (St-0, St-1, St-3 and St-5) for radionuclides and metal concentrations, bacterial abundance, physiological diversity of microbial community (Shannon index Hp), substrate richness (number of wells with OD higher than 0.25) and evenness (Pielou index, E), and observed OTUs, richness (Chao 1) and diversity (Shannon index H′) of the bacterial and fungal communities were analyzed by univariate analysis using a Kruskal-Wallis non parametric test followed by pairwise comparison test using Tukey contrast ($P < 0.05$) using the "*nparcomp*" package of R software (Konietschke et al., 2015). Pearson correlation coefficient was used to test whether there is significant relationship between community level physiological profiles (CLPPs) and organic matter (total Carbon Ct, total nitrogen Nt) and iron (Fe) and available fraction of radionuclides and metals (Cu, Pb, Zn, ^{238}U, ^{226}Ra, ^{210}Po).

Sparse Partial Least Squares Discriminant Analysis (sPLS-DA) was performed to select discriminant OTUs between different sites using the function "*splsda*" from the "*mixOmics*" package (Rohart et al., 2017). The optimal number of component and variables (= OTUs) to include in the model was achieved using the "*tune.splsda*" function on centroid distances and was validated by Mfold cross-validation (folds = 3, repeat = 50). Then, a partial least square regression (PLSr) analysis was performed to determine the relationships between the resulting discriminant OTUs' abundance (bacteria and fungi) and the different groups of parameters, including: i) organic matter and iron (total Carbon Ct, total nitrogen Nt, Organic Matter OM, clay, Fe) and ii) available fraction of radionuclides and metals (Cu, Pb, Zn, ^{238}U, ^{226}Ra, ^{210}Po). In addition, the weight of each metal or radionuclide parameter was determined in the variation in bacterial or fungal "abundances". All statistical analyses were computed using R software (R Core Team, 2021) (https://www.R-project.org/).

All raw sequences used in this study are available in the sequence read archive (SRA) at NCBI database under the accession number PRJNA996897.

3. Results

3.1. Characterization of stream water and sediments

The composition of stream water was rather similar between sites (see Table S1 for details). The oxidizing potential ranged from 80 to 119 mV (with respect to the normal hydrogen electrode (NHE)), temperature and conductivity were relatively low (5.4–7.3 °C and 47–60 µS.cm^{-1} respectively) and the average composition was globally constant. Only the pH displayed slight differences between sites, with values of 6.4, 6.2,

Table 1
(A) Total mass activity of some radionuclides in the sediment (Bq.kg^{-1}, dry weight); except for the case of Po-210 (alpha analysis), and for U-238 and Th-232 (activities calculated from the concentration measured by ICP-MS, Table 1B) the data are from the gamma analyses. (B) concentration of trace elements in the sediments measured by ICP-MS (mg.Kg^{-1}).

A

		U-238 decay chain				U-235 decay chain		Th-232 decay chain		
	U-238	Th-234	Ra-226	Po-210	Pb-210	U-235	Ac-227	Th-232	Ra-228	Th-228
Samples	Bq.Kg^{-1}									
St-0	368 ± 47	140 ± 12	251 ± 14	309.6 ± 15.1	138 ± 13	6.1 ± 3.8	6.2 ± 2.0	30 ± 3	55.5 ± 5.2	39.6 ± 3.0
St-1	808 ± 104	576 ± 44	970 ± 135	463.2 ± 22.0	303 ± 25	26.6 ± 8.4	24.3 ± 4.5	27 ± 5	116 ± 10	64.8.6 ± 5.0
St-3	1710 ± 218	1029 ± 76	2421 ± 122	1225.9 ± 47.7	799 ± 59	51.3 ± 12.8	46.0 ± 6.8	79 ± 2	140 ± 13	103 ± 8
St-5	1625 ± 208	1145 ± 83	1704 ± 137	1471.0 ± 54.8	1137 ± 83	55.5 ± 8.9	43.0 ± 4.9	62 ± 4	123 ± 11	76.0 ± 5.6

B

	U	Th	As	Pb	Cu	Zn	Fe
Samples	mg.Kg^{-1}						
St-0	29.6 ± 3.8	7.3 ± 0.6	601 ± 29	152 ± 10	9.5 ± 0.3	19.8 ± 8.0	60,259 ± 3475
St-1	64.9 ± 5.0	6.5 ± 1.1	391 ± 6	192 ± 10	7.8 ± 0.8	13.4 ± 7.0	51,607 ± 3641
St-3	136.7 ± 7.6	19.5 ± 0.6	449 ± 14	405 ± 26	15.2 ± 1.2	144 ± 13	72,218 ± 365
St-5	130.6 ± 7.6	15.3 ± 0.9	165 ± 8	441 ± 54	16.6 ± 0.1	123 ± 10	30,511 ± 225

5.4 and 7.3 for St-0, St-1, St-3 and St-5, respectively. Trace element concentrations were overall below the limit of quantification, and uranium values were 0.7 and 2.6 mg.kg^{-1} in sites St-0 and St-1and 1.9 and 1.6 mg.kg^{-1} in St-3 and St-5 (detail is provided in Table S1).

Regarding the sediments, X-ray diffraction indicated the presence of an altered granitic rock with the presence of quartz, K-feldspar and plagioclase as well as a clay phase mainly composed of illite-mica, chlorite and kaolinite (see Table S2 for details). The most downstream sampling sites (St-3 and St-5) exhibited greater proportions of clay (~35 % of clay especially swelling clays (smectite and/or interstratified illite/smectite ~7 %) compared to ~13 % for St-0 and St-1) and quantity of organic matter (~58 g(C).kg^{-1} compared to ~16 g(C).kg^{-1} for St-0 and St-1).

Regardless of the measured radionuclides, mass activity values (Bq.kg^{-1}) were higher in the downstream sampling sites (St-3 and St-5) compared to the upstream ones (St-0 and St-1) (Table 1A). In the ^{238}U and ^{235}U and ^{232}U decay chains, the RNs activities were in the same order of magnitude. Converting the quantity of Th measured by ICP-MS (Table 1B) in Bq.kg^{-1} led to values similar than those measured by gamma spectrometry for ^{228}Ra and ^{228}Th (Table 1). This indicates a global secular equilibrium in the chain. However, the calculated activities for ^{238}U were significantly different to the mass activities measured for ^{234}Th, the radionuclide in secular equilibrium with ^{238}U; i.e. the activity measured for ^{234}Th should correspond to the activity of ^{238}U (Table 1). The differences observed are certainly due to the different samples used for the analysis; although taken from the same place, the possibility of a slight heterogeneity cannot be ruled out since the quantity measured by gamma spectrometry (60-90 g) was much higher than the one used for the ICP-MS analysis after digestion (0.5 g). For the statistical analyses, the data obtained by ICP-MS were used.

The results of ERICA tool, considering 1 Bq.kg^{-1} for each RN, indicated that the internal dose rate of RNs represented >83 % of the total dose rate for phytoplankton (Detail is provided in Table S3). For these kinds of organisms, the main contributors to the internal dose were uranium isotopes, ^{235}U and ^{238}U, as well as, ^{226}Ra and ^{210}Po, all of them being alpha-emitters. The internal dose rates due to these four RNs represented >99 % of the internal dose rates.

Based on ICP-MS analyses, toxic elements such as As, Pb, Cu and Zn were found in significant quantities in the sediments and were therefore considered to potentially impact microorganisms (Table 1B). Arsenic was measured in significant quantities in all the samples, with higher concentration values at the reference sampling site (St-0, 601 mg.Kg^{-1}) compared to the most downstream site (St-5, 165 mg.Kg^{-1}). This resulted in the absence of correlation between Arsenic and radioactivity contamination. In the case of lead, the quantity increased with the concentration of radionuclides with values that varied between ~150 and ~ 440 mg.Kg^{-1}. A globally similar trend was observed for Cu (~8–17 mg.Kg^{-1}) and Zn (~14 and 140 mg.Kg^{-1}). For iron (Table 1B) their values were very high (ranging from 30 to 72 g.Kg^{-1}) but lower in St-5.

The sequential extraction procedure employed in this study allowed the construction of a detailed profile of the potentially available trace elements and the physico-chemical perturbations that might destabilize them. The release of trace elements in steps 1 to 5 provide an estimation of the bioavailable fraction potentially mobilized under various conditions: leaching with circumneutral stream water, mild acidic conditions, acidic conditions, reducing Eh conditions, and strongly oxidizing conditions. The residual fraction (i.e. that remain in the rock matrix after these five extraction steps) reflect the amount of trace elements irreversibly trapped and therefore considered not available for organism uptakes.

Although the majority of trace elements measured accumulated mainly in the residual fraction, with Th and As found exclusively in the residual part, significant amounts were also detected in the potentially bioavailable fractions (Table 2). This was the case for Pb (11–30 % in the F1-F5 fractions with the majority found in F3), ^{210}Po (5–14 % in the F1-

Table 2
Percentages of the different fractions of radionuclides/radioelements, toxic trace elements, heavy metals and Fe obtained by the sequential extraction. For each element, the potentially bioavailable fractions (F1: water soluble, F2: exchangeable, F3: bound-to-carbonates, F4: bound-to-iron and manganese oxides, F5: bound-to-organic matter), their specific contribution (> 5 % of the total amount – Main reservoir) and the residual fraction (F6) are displayed (mean ± SEM) for each point (St-0, St-1, St-3 and St-5).

	Th		U		Ra-226		Po-210		Cu		As		Pb		Zn		Fe	
	F1-F5	Residual	F1-F5	Main reservoir(s) (F1-F5)	Residual	F1-F5*	Residual	F1-F5	Main reservoir(s) (F1-F5)	Residual	F1-F5	Residual	F1- F5	Main reservoir(s) (F1-F5)	Residual	F1-F5	F1- F5	Main reservoir(s) (F1-F5)	Residual
	%		%		%		%		%		%		%		%		%		
St-0	<DL	86 ± 34	58 ± 13	F3;43 ± 0.5 F5;8.3 ± 0.3	32 ± 5	54 ± 28	46 ± 24	8.2 ± 3.6	-	91.8 ± 1.1	18.1 ± 0.2 (F5)	83 ± 5	<DL	101 ± 7	11.2 ± 0.3	95 ± 8	<DL	<LD	9.2 ± 1.1	F3;5.7 ± 0.3	92 ± 8
St-1	<DL	89 ± 38	73 ± 7	F2;5.2 ± 0.3 F3;39.5 ± 0.4 F4;8.9 ± 0.6 F5;19.5 ± 0.3	22 ± 2	29 ± 4	71 ± 10	14 ± 7	F3;9.1 ± 0.9	86.1 ± 2.3	25.2 ± 0.3 (F5)	90 ± 16	<DL	100 ± 2	18 ± 2	F3;17.3 ± 0.3	87 ± 5	<DL	<LD	15.8 ± 3.0	F3;9.0 ± 0.4	85.4 ± 8.2
St-3	<DL	101 ± 4	80 ± 18	F3;50 ± 5 F5;12.3 ± 0.5	21.5 ± 1.6	16 ± 2	84 ± 9	4.6 ± 1.9	-	95.4 ± 5.0	5 ± 1 (F5)	96 ± 11	<DL	101 ± 5	15.2 ± 2.2	F3;14.5 ± 1.1	80 ± 5	<DL	82 ± 24	11.6 ± 2.1	F3;5.3 ± 0.1 F5;5.0 ± 0.9	89.5 ± 1.8
St-5	<DL	91 ± 6	77 ± 12	F2;7.2 ± 0.5 F3;59 ± 5 F5;8 ± 1	24.2 ± 1.5	61 ± 19	39 ± 12	8.0 ± 2.2	F3;5.7 ± 0.3	92.0 ± 1.8	52.7 ± 3.8 (F5)	48.5 ± 3.8	<DL	101 ± 7	30 ± 3	F3;29 ± 3	63 ± 11	<DL	60 ± 20	13.0 ± 2.5	F3;7.3 ± 0.2	88.2 ± 2.0

* Difference between the total quantity and that measured in F6.

Table 3
Bacterial abundance (10^{10} cell g^{-1} dry weight), observed OTUs, richness (Chao 1), diversity (Shannon index H′) and OTU coverage (%) of bacterial and fungal communities from sediment samples, average well color development (AWCD), bacterial community level physiological profiles (CPPLs,) expressed as rate (rj^{-1}) of consumption of the groups of substrates (CA: carboxyl acids, PL: polymers, CH: carbohydrates, AA: amino acids, AM: amines), indices of diversity (Hp) and eveness (E) calculated on CPPL.

Samples	10^{10} cell g^{-1} DW	Observed OTUs		Chao 1		Shannon H′		Coverage (%)		AWCD	CLPP ($r = j^{-1}$)				Hp	E
		Bacteria	Fungi	Bacteria	Fungi	Bacteria	Fungi	Bacteria	Fungi		CA	PL	CH	AA	AM	
St-0	3.05 ± 9.3 10^{9}	487	325 ^{a}	553	565 ^{a}	5.56	3.51 ^{a}	0.97	0.97	1.72 ± 0.17	0.32 ± 0.04	0.26 ± 0.06	0.72 ± 0.07 ^{a}	0.24 ± 0.02 ^{a}	0.33 ± 0.03 ^{a}	3.21 ± 0.03	0.96 ± 0.00
St-1	6.90 ± 1.7 10^{9}	504	422 ^{a}	585	666 ^{a}	5.52	4.30 ^{ab}	0.97	0.96	1.62 ± 0.14	0.33 ± 0.02	0.37 ± 0.07	0.86 ± 0.02 ^{b}	0.38 ± 0.08 ^{a}	0.36 ± 0.16 ^{a}	3.23 ± 0.07	0.98 ± 0.01
St-3	8.44 ± 5.4 10^{8}	512	631 ^{b}	574	867 ^{b}	5.79	5.12 ^{ab}	0.97	0.95	1.57 ± 0.13	0.30 ± 0.01	0.36 ± 0.01	0.43 ± 0.01 ^{c}	0.34 ± 0.03 ^{a}	0.49 ± 0.03 ^{ab}	3.24 ± 0.05	0.98 ± 0.01
St-5	8.48 ± 3.1 10^{10}	497	596 ^{b}	555	863 ^{b}	5.76	4.43 ^{b}	0.98	0.95	1.61 ± 0.06	0.30 ± 0.01	0.27 ± 0.01	0.21 ± 0.02 ^{d}	0.09 ± 0.01 ^{b}	0.17 ± 0.02 ^{ac}	3.23 ± 0.05	0.98 ± 0.01

Data are presented as mean ± standard deviation ($n = 3$). Means followed by same superscript or without superscript within column are not significantly different at $p < 0.05$.

F5 fractions with the majority found in F3), Fe (9–16 % in the F1-F5 fractions, with the majority found in F3) and Cu (5–53 % in the F1-F5 fractions with the majority found in F5). The Zn content in the F1-F5 fractions was always below the detection limit. Only the fraction F6 was measurable in sites St-3 and St-5, suggesting that the majority of Zn was likely non-available (~80 %). Drawing from these observations and the consistent patterns of the other elements across fractions at the different sampling sites (with the exception of Ra), a fraction of available Zn of 20 % was considered for statistical analyses in St-0 and St-1 (Table 2). The ultimately most available element was uranium; it is the element for which the residual fractions were the least important (22–32 %), and which was found in two main fractions (F3 and F5). Finally, ^{226}Ra appeared to be a somewhat special case, with a potentially bioavailable portion that varied from 16 to 61 % depending on the point considered (Table 2). The bioavailable fractions of U, Ra, Pb, Cu and Fe tended to be higher in the most downstream sites (St-3 or St-5).

3.2. Microbial communities' structure in the sediment samples

A total of 231,259 and 289,055 reads were obtained using NGS sequencing for bacteria and fungi respectively (MiSeq Illumina sequencing) leading to 139,244 and 287,214 sequences after quality control. The number of sequences per sample for bacteria and fungi were respectively of 3396 and 4922 for a total of 735 and 1823 OTUs.

Based upon these results, three alpha diversity indexes (Chao1, Shannon and Coverage) were calculated to evaluate the richness, diversity and coverage of the microbial communities (Table 3). Concerning bacteria, no statistical differences were observed between the different sampling sites, neither in terms of alpha diversity indexes nor in terms of OTUs richness. Nevertheless, bacterial abundances, as measured by flow cytometry, tended to be higher in sites St-3 and St-5 (respectively 8.44 10^{10} ± 5.4 10^{8} and 8.48 10^{10} ± 3.1 10^{10} cell.g^{-1} DS) compared to sites St-0 and St-1 (respectively 3.05 10^{10} ± 9.3 10^{9} and 6.9 10^{10} ± 1.7 10^{9} cell.g^{-1} DS, Table 3). Concerning fungi, highest Chao1 richness estimator values were observed for sampling sites St-3 and St-5 (respectively 867 and 863) compared to sites St-0 and St-1 ($P < 0.05$, respectively 565 and 666) (Table 3). These values were higher than those of bacterial one's. For Shannon index, the fungal diversity was also higher in site 5 ($H' = 4.43$) and significantly different from the reference site (St-0 = 3.51, $P < 0.05$). Fungal diversity was low compared to the bacterial one's.

Among the 12 bacteria phyla observed for the 4 sampling sites, *Proteobacteria* was the most dominant one, (ranging 40.4 % to 49.5 % of total bacterial sequence reads) (detail is provided in Fig. S2) followed by *Bacteroidetes* (14.1 % - 30.8 % in St-0 and St-5 respectively) and *Cyanobacteria* (16.7 %, mostly in St-1). Additionally, *Acidobacteria*, *Nitrospirae*, *Actinobacteria*, *Verrucomicrobia*, *Planctomycetes*, *Chloroflexi*, *Spirochaetae* and *Deinococcus-thermus* were detected in all the samples, although they represented <10 % of the relative abundance. Regarding fungi, 5 main phyla were identified in the samples, dominated by *Ascomycota* (57.4 % - 77.0 % in St-3 and St-1 respectively), followed by *Basidiomycota* (10.3–34.6 % in St-5 and St-0 respectively) and *Glomeromycota* (8.1 %, moslty in St-3) (detail is provided in Fig. S3).

Beta-diversity wise, sediment samples from sites St-3 and St-5 differed significantly from one another while those of sites St-0 and St-1 were similar (Figs. 2B and 3B). The sparse PLS-DA used in this study allowed to highlight the main bacterial and fungal OTUs that discriminated these sampling sites. Regarding bacteria (Fig. 2A), 16 specific OTUs mostly *Burkholderiales* (*Acidovorax sp*, *Rhodoferax* sp. and *Roseateles* sp.), *Marinibacteriales* (*Mangroviflexus* and *Prolixibacter*), *Nostocales*, *Methylococcales* (*Crenotrix) and Acidibacter* orders, were more abundant in sediment of sampling site St-5. Additionally, 87 different OTUs were more abundant in sampling site St-3 compared to the other sites. These were mainly *Acidobacteriales* (*Acidobacteria* phylum), *Rhodocyclales* and *Nitrosomonadales* (*Betaproteobacteria* phylum), *Rhizobiales* and *Sphingomonadales* (*Alphaproteobacteria* phylum) orders among other (Fig. 2A).

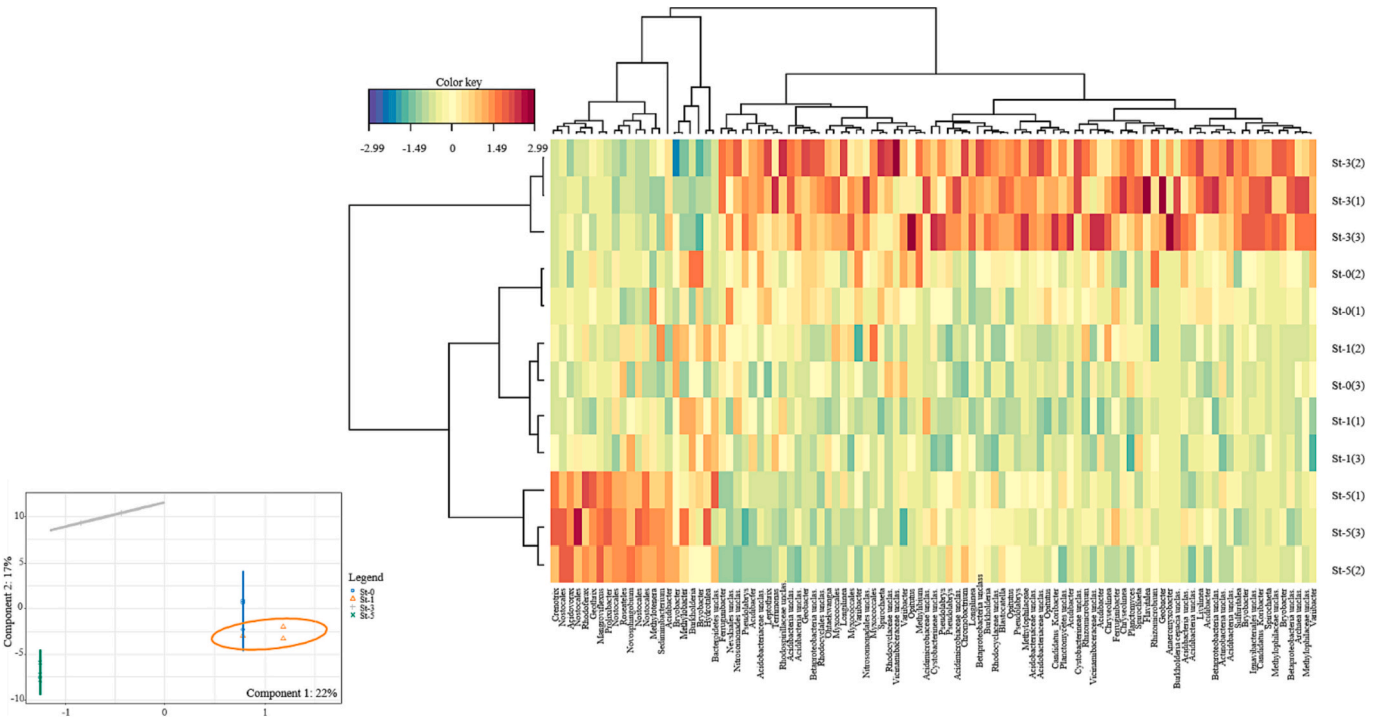

Fig. 2. sPLS-DA analysis (A) on the bacterial community composition in the 4 different sediment samples (St-0, St-1, St-3, St-5) (95 % confidence level ellipse plots). Heatmap plot (B) representing the relative abundances of OTUs picked up using sPLS-DA in columns and samples in rows.

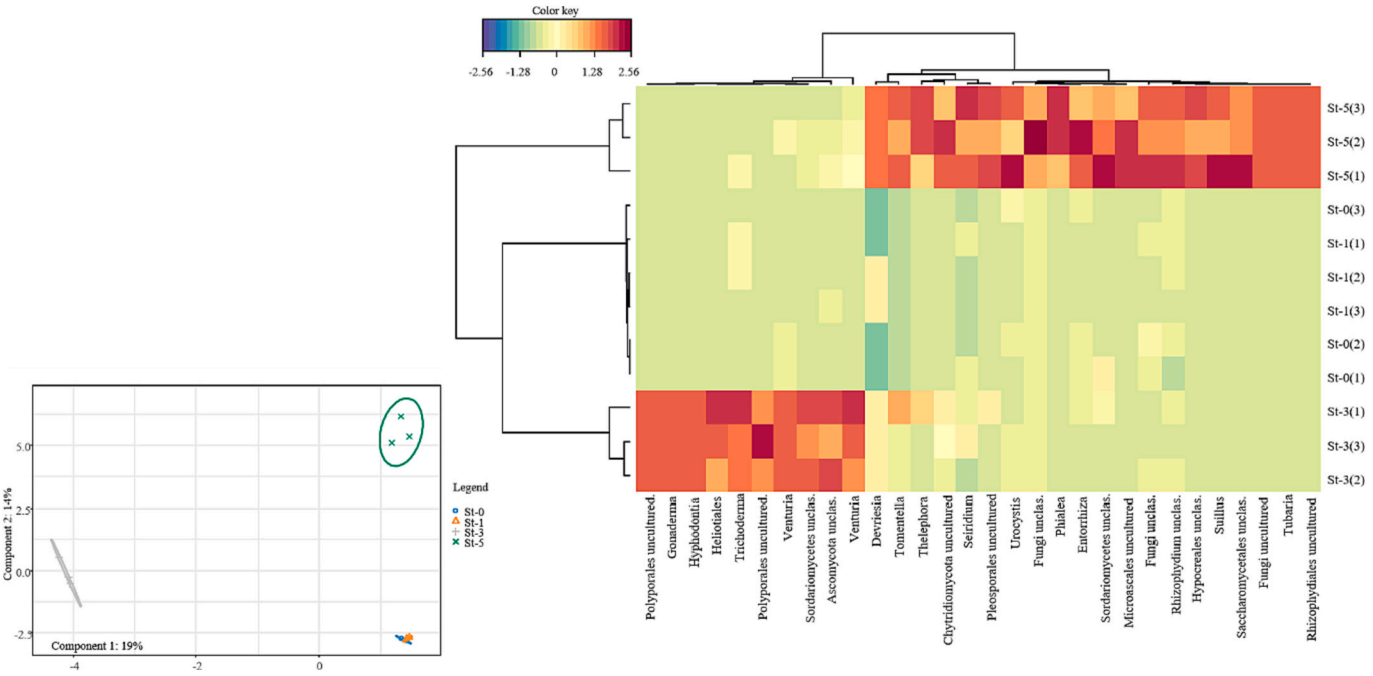

Fig. 3. sPLS-DA analysis (A) on the fungal community composition in the 4 different sediment samples (St-0, St-1, St-3, St-5) (95 % confidence level ellipse plots). Heatmap plot (B) representing the relative abundances of OTUs picked up using sPLS-DA in columns and samples in rows.

Concerning fungi (Fig. 3A), *Pleosporales* and *Capnodiales* (*Dothideomycetes* class), *Helotiales* (*Leotiomycetes* class), *Xylariales* and *Hypocreales* (*Sordariomycetes* class) orders belonging to the Ascomycota, as well as *Agaricomycetes* (*Polyplorales*, *Thelephorales*, *Boletales*, *Agaricales* orders) and *Chytridiomycota* (*Rhizophydiales* order) belonging to the *Basidiomycota*, were more abundant in sampling site St-5. Conversely, ten fungal OTUs were found to be more abundant in sampling site St-3 compared to the other sites (Fig. 3B). These were affiliated to *Helotiales* (*Leotiomycetes* class), *Hypocreales* (*Sordariomycetes* class), *Venturiales* (*Dothideomycetes* class), *Polyporales* and *Hymenochaetales* (*Agaricomycetes* class) orders.

Such differences in bacterial and fungal assemblages between sampling sites could be associated with the differences in the physical and chemical properties of the sediments as previously mentioned and especially ^{238}U, ^{226}Ra, ^{210}Po, Pb, Cu and OM (Figs. 4B, 5B). While these bioavailable forms of radionuclides and Cu are expected to be toxic to microorganisms, positive relationships were observed with several

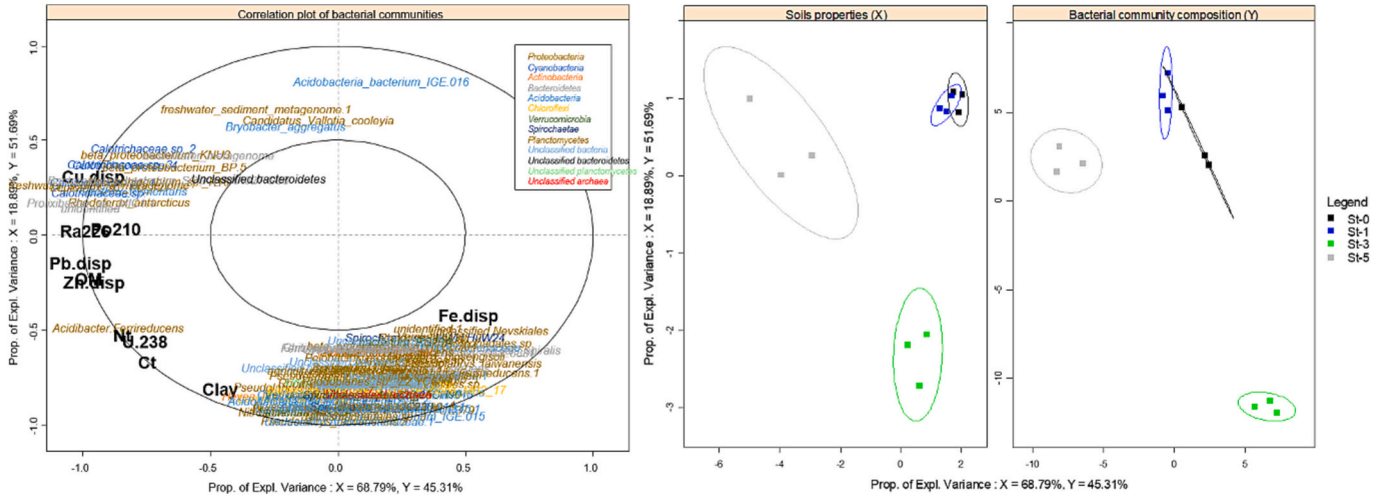

Fig. 4. Partial least square regression (plsr) correlation plot between bacterial community structure and physical and chemical properties of soils from the different sampled sites (A). Soil's properties (including radionuclide concentrations) are indicated in black whereas the different bacterial phyla are indicated by the color code. Scatter plot of individuals (sampled sites) for both soil properties (= X block) and bacterial community composition (= Y block) (B). The different sampling sites are highlighted by the color code and statistical differences between sites are assessed by 95 % level confidence ellipses.

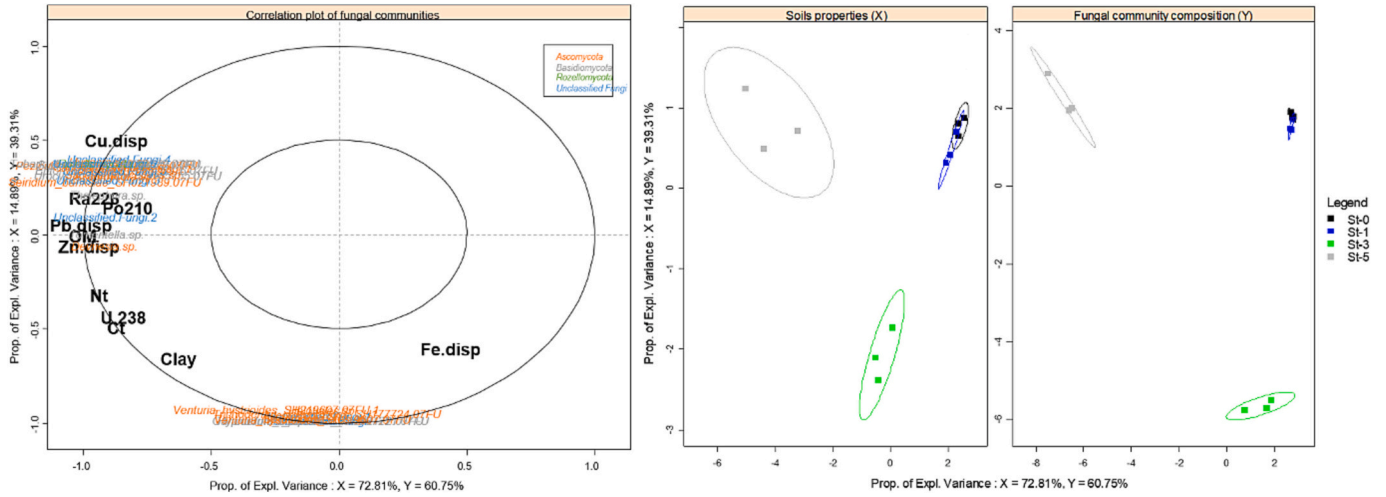

Fig. 5. Partial least square regression (plsr) correlation plot between fungal community structure and physical and chemical properties of soils from the different sampled sites (A). Soil's properties (including radionuclide concentrations) are indicated in black whereas the different fungal phyla are indicated by the color code. Scatter plot of individuals (sampled sites) for both soil properties (= X block) and bacterial community composition (= Y block) (B). The different sampling sites are highlighted by the color code and statistical differences between sites are assessed by 95 % level confidence ellipses.

microbial species. Specifically, many bacterial OTUs, including, *Beta-proteobacteria* (*Acidovorax*, *Rhodoferax*, *Roseateles*, *Methylotenera*) *Nostocales*, *Bacteroidetes* (*Prolixibacter*, *Sediminibacterium* and *Mangroriflexus*) and secondary *Alpha-* and *Gamma-proteobacteria* (respectively *Novosphingobium* and, *Crenotrix* and Acidibacter) and *Acidobacteria* (*Geothrix*) dominant at site 5, were positively related with concentrations of ^{226}Ra, ^{210}Po, Pb, Cu and OM (Fig. 4A). Conversely, concentrations of Fe and ^{238}U, clay, carbon and total nitrogen were positively related to *Acidobacteria* (mainly *Bryobacter*), *Bacteroidetes* (*Chryseolinea*, *Hydrotalea*, *Ferruginibacter*), *Chlorofexi* (*Longilinea*, *Levilinea*), *Alphaproteobacteria* (*Rhizomicrobium*, *Pseudolabrys*, *Variibacter*), *Betaproteobacteria* (mainly Rhodocyclaceae), *Deltaproteobacteria* (*Geobacter*, *Myxoccocales*), *Gammaproteobacteria* (*Acidibacter*) and *Spirochaetes*, dominant at site 3. Concerning fungi (Fig. 5A), many fungal OTUs (*Ascomycota*, *Dothideomycetes*: *Deviesia*, *Pleosporales*; *Sordariomycetes*: *Seiridium*, and *Basidiomycota*, *Agaricales*: *Thelephorales*: *Thelephora*, *Tomentella*) displayed a positive relationship with concentrations of available fraction of Cu, Pb, Zn, ^{226}Ra, high concentration of organic matter and total nitrogen, typical of sampling site St-5. In site St-3, the majority of Ascomycetes are positively correlated with bioavailable iron and clay concentrations.

Regarding the Average Well Color Development (AWCD) there were no difference between sampling sites. However, they were differences in carbon sources utilization (CLPPs) (Table 3). Specifically, the rates of consumption of carbohydrates, the most widely used carbon sources, tended to decrease along the pollution gradient as they were significantly lower in St-3 and St-5 compared to the others ($P < 0.05$). The rate of consumption of amino acids, the less used substrate, was also significantly lower in St-5 compared to the others ($P < 0.05$). The bacterial physiological diversity estimated by Shannon index (Hp) remained stable in all the sediment samples (between 3.21 ± 0.03 and 3.24 ± 0.05).

4. Discussion

The aim of the study was to assess the potential impact of exposure to

radionuclides (RN) and heavy metals associated with a former mining activity, on microorganisms in stream sediments characterized by a contamination gradient from upstream to downstream.

With the exception of organic matter and clay content, similar trends in sediment physico-chemical composition were observed between sampling sites. Organic matter, higher in the most contaminated sites, plays an important role in the mobility of heavy metals and radionuclides) and for microorganisms (Ding et al., 2019; Ma et al., 2020). Because of the radiation they emit, radionuclides can exert different effects on microorganisms: one related to the external dose (mainly gamma radiation) and the other related to the internal dose (mainly alpha and beta radiation, particularly in cases of internal incorporation). The results of the ERICA tool indicated that this size of microorganisms was considerably exposed internally to ^{226}Ra, ^{210}Po, ^{235}U and ^{238}U whereas the external dose could be neglected. It is on the basis of these results that our assessment was conducted. However, as this reference radioecological tool does not support evaluations at the micrometric scale (Ulanovsky and Pröhl, 2006), the dose rates to microorganisms should be handled prudently and be complemented with Monte Carlo simulation tools (Kolovi et al., 2023). To be as realistic as possible, RNs bioavailable fraction (Chandwadkar et al., 2018; Sitte et al., 2015), evaluated by sequential extraction (F1-F5), was considered. The same applies to toxic elements and iron, for which a bioavailable fraction could be measured. Note that in the proposed approach, we make the implicit assumption that the entire bioavailable reservoir is accessible through the interstitial water by microorganisms, which can locally generate significant physico-chemical disturbances.

The main hypothesis was that available radionuclides and heavy metals carried by stream water and accumulating for a long time (69 years) in the sediment of the wet zone would not induce drastic changes in the diversity of microbial species but rather influence its composition. Here, similar bacterial diversity indices (abundance and α-diversity index) were observed along the gradient of contamination from upstream to downstream, whereas fungi appeared stimulated as shown by the higher diversity and richness observed downstream. The long-term chronic exposure of bacteria and fungi to significant fraction of bioavailable radionuclides and heavy metals most likely selected for the most resistant and/or tolerant microorganisms to the detriment of the sensitive ones (Fashola et al., 2016; Sitte et al., 2015; Zhao et al., 2019). Moreover, the higher concentration of OM downstream may have mitigated the toxic effects of radionuclides, along with the opening of new ecological niches. OM can also participate in the stimulation of microbial metabolic processes involved in the speciation of metalloids and radionuclides and therefore in the reduction of their toxicity (Violante et al., 2010). Nevertheless, the reduction in the degradation of carbohydrates (CH), amino-acids (AA) and amines (AM) (Table 4) and the negative correlations between Pb and carbohydrates or AA (−0.872 and − 0.730 respectively, $P < 0.05$), Cu and AA or amines, (−0.909 and − 0.775 respectively, $P < 0.05$) and between U and carbohydrates (−0.833, $P < 0.05$) suggest that several microbial functions carried by bacteria and related with carbon and nitrogen cycling may have been impaired (Kenarova et al., 2014). This was even more striking at the most downstream sampling site (St-5), where uranium and heavy metals concentrations were the highest.

Fungi are known to possess a large panel of extracellular enzymes, of which ligninolytic ones' act as key players in the decomposition of recalcitrant compounds (*Thelephora* and *Tomentella*), providing them with nutrients and energy (Rosales-Castillo et al., 2017). The fact that these fungal OTUs (*Sordariomycetes* and *Agaricomycetes* (*Thelephora* and *Tomentella*)) were found in greater abundance in the most contaminated sites and significantly positively related to available Cu, Pb, Zn and ^{226}Ra highlights that the community likely shifted toward more adapted/tolerant fungal taxa to radionuclides and heavy metal excess (Hui et al., 2011; Kujala et al., 2018; Regvar et al., 2010). Indeed, these positive relationships indicate that these microorganisms tolerate or use these elements as it had been supposed (Pennanen et al., 1996; Narendrula-Kotha and Nkongolo, 2017). The surface of fungal cells contains chitin, known for its high capacity to remove heavy metal ions (Gadd, 1986). Furthermore, the specific detection of filamentous fungi, (i.e. *Dothideomycetes*) highlight the ability of some microbial species to enhance the adhesion of biofilms to sediment due to an increase rigidity and organization, in turn affecting the development of other microbial species. This may favor the development of species less tolerant to metals within microbial assemblages, explaining the contradiction observed with our results, where high concentrations of trace elements did not decrease fungal diversity, despite their reported sensitivity to contamination (Pan et al., 2020; Stępniewska et al., 2020). This contradiction can also be explained by the fact that the total quantities of contaminants were considered in previous assessments, not just the available one. *Agaricomycetes* are known substantial contributors in nutrient turnover and shifts in the proportions of their trophic guilds (ectomycorrhizal and saprophic) due to association of biotrophy with increased tolerance to pollution may have huge consequences at the ecosystem level (carbon and nitrogen dynamics) (Mikryukov et al., 2020).

The long time exposure involve various resistance mechanisms, either inherent or acquired (Beattie et al., 2018), such as biosorption, precipitation, accumulation (Beazley et al., 2007; Choudhary and Sar, 2011; Merroun et al., 2005; Zafar et al., 2007) and modification of the redox state of uranium. The enrichment of *Geobacter, Myxococcales* (*Deltaproteobacteria*), *Acidibacter* (*GammaProteobacteria*), *Chloroflexi* (*Anaerolineae*), *Sediminibacterium* and *Prolixibacter* (*Bacteroidetes*) in St-5, as previously observed in enriched U sediments (Sutcliffe et al., 2018; Zeng et al., 2020), and their positively correlations with the available fraction of radionuclides (^{238}U, ^{226}Ra, ^{210}Po) and heavy metals (Cu, Pb) certainly highlights such phenomenon. High concentrations of available copper in this site could benefit to *Geothrix*-like OTUs for their respiration (Sutcliffe et al., 2019). The ability of all these bacteria to reduce or mineralize available uranium have already been reported (Kazy et al., 2009; Merroun et al., 2005, 2011). Other examples such as *Myxococcales*, positively correlated with the available fraction of Cu and U in this study, was known to form insoluble metal-sulphide complexes of dissolved metals such as U(VI) (Yin et al., 2019). ^{238}U and ^{226}Ra mainly in bioavailable fraction in the most contaminated site, may be also immobilized by biosorption or accumulation with the phosphate groups of lipopolysaccharides in the cell wall of *Acidovorax* sp. and *Rhodoferax* (*Betaproteobacterai*) (Krawczyk-Bärsch et al., 2018) or *Cyanobacteria* and more specifically *Nostocales* order (Heidari et al., 2018). The tolerance of *Nostocales* could be due to their cell surfaces, which excrete exopolymeric substances (EPS), or their intracellular polyphosphates, which can also concentrate metal ions and ^{238}U or ^{226}Ra (Mehta et al., 2019).

5. Conclusion

In this work, a comprehensive methodology is proposed to assess the impact of contaminations on microbial communities in sediments impacted by past uranium mining activities. It considers the entire environment, including composition, physico-chemical parameters, and the content of trace metals and radionuclides. For the radioactivity component, the ERICA model serves as a working tool, indicating that external radiotoxicity can be neglected based on the activities found in the sediments. Regarding internal (radio)toxicity, it was accounted for in the case of relevant radionuclides (^{238}, ^{235}U, ^{226}Ra, ^{210}Po) and toxic metals (Cu, Pb, Zn) through the evaluation of bioavailable fractions assessed by sequential extraction.

The key outcome of this work revealed that long-term contamination with radionuclides (^{238,} ^{235}U, ^{226}Ra, ^{210}Po) and heavy metals (Cu, Pb, Zn) significantly impacted the composition of the microbial community, rather than its diversity. The selective pressure induced by ^{238}U, ^{226}Ra, Cu and Pb, the most available radionuclides and heavy metals, on bacteria and fungi causes native microbial communities to evolve toward to

composition dominated by resistant species, leading to communities tolerant to site-specific levels of contamination. Several microbial functions carried by bacteria and related with carbon and nitrogen cycling have also been impaired. Nevertheless, in these natural conditions, it was not possible to discriminate which of heavy metals and radionuclides had the greatest effect on the bacterial and fungal communities. Furthermore, this work demonstrates that organic matter is an important parameter to consider since it also significantly alters, either directly or indirectly, the bacterial and fungal composition. Microorganisms can interact directly with the bioavailable fractions of contaminants and thus reduce their effects, but OM can also affect the bioavailability of contaminants by modifying their speciation.

Funding

This work was supported by the French "Cellule Energie du CNRS, NEEDS-Nucléiare, Energie, Environnement, Déchets et Société, Projet fédérateur Environnement" under Tremplin project.

CRediT authorship contribution statement

Clarisse Mallet: Conceptualization, Funding acquisition, Investigation, Project administration, Supervision, Writing – original draft, Writing – review & editing. **Florent Rossi:** Formal analysis, Writing – original draft, Writing – review & editing. **Yahaya Hassan-Loni:** Investigation, Resources, Writing – review & editing. **Guillaume Holub:** Investigation, Writing – original draft, Writing – review & editing. **Le Thi-Hong-Hanh:** Writing – review & editing. **Olivier Diez:** Investigation, Resources. **Hervé Michel:** Investigation, Methodology, Writing – original draft, Writing – review & editing. **Claire Sergeant:** Investigation, Resources, Writing – original draft. **Sofia Kolovi:** Methodology, Writing – review & editing. **Patrick Chardon:** Methodology, Resources, Writing – review & editing. **Gilles Montavon:** Conceptualization, Investigation, Supervision, Writing – original draft, Writing – review & editing.

Declaration of competing interest

The authors declare that they have no known competing financial interests or personal relationships that could have appeared to influence the work reported in this paper.

Data availability

Data will be made available on request.

Acknowledgments

The authors are grateful to the ZATU Pilot Workshop within the Hercynian orogeny (ZATU, https://zatu.org/).

BRGM is thanked for the analyses carried out by XRD and J. Champion (Subatech) for her contribution to data acquisition.

Thanks are also extended to Courson Olivier with IPHC Strasbourg for Qgis maps.

References

Abdelouas, A., 2006. Uranium mill tailings: geochemistry, mineralogy, and environmental impact. Elements 2, 335–341. https://doi.org/10.2113/gselements.2.6.335.

Beattie, R.E., Henke, W., Campa, M.F., Hazen, T.C., McAliley, L.R., Campbell, J.H., 2018. Variation in microbial community structure correlates with heavy-metal contamination in soils decades after mining ceased. Soil Biol. Biochem. 126, 57–63. https://doi.org/10.1016/j.soilbio.2018.08.011.

Beazley, M.J., Martinez, R.J., Sobecky, P.A., Webb, S.M., Taillefert, M., 2007. Uranium biomineralization as a result of bacterial phosphatase activity: insights from bacterial isolates from a contaminated subsurface. Environ. Sci. Technol. 41, 5701–5707. https://doi.org/10.1021/es070567g.

Bernard, M., Rué, O., Mariadassou, M., Pascal, G., 2021. FROGS: a powerful tool to analyse the diversity of fungi with special management of internal transcribed spacers. Brief. Bioinform. 22, bbab318 https://doi.org/10.1093/bib/bbab318.

Bernhard, G., Geipel, G., Brendler, V., Nitsche, H., 1998. Uranium speciation in waters of different uranium mining areas. J. Alloys Compd. 271–273, 201–205. https://doi.org/10.1016/S0925-8388(98)00054-1.

Blankenberg, D., Kuster, G.V., Coraor, N., Ananda, G., Lazarus, R., Mangan, M., Nekrutenko, A., Taylor, J., 2010. Galaxy: a web-based genome analysis tool for experimentalists. CP Mol. Biol. 89 https://doi.org/10.1002/0471142727.mb1910s89.

Boteva, S., Radeva, G., Traykov, I., Kenarova, A., 2016. Effects of long-term radionuclide and heavy metal contamination on the activity of microbial communities, inhabiting uranium mining impacted soils. Environ. Sci. Pollut. Res. 23, 5644–5653. https://doi.org/10.1007/s11356-015-5788-5.

Bresson, C., Ansoborlo, E., Vidaud, C., 2011. Radionuclide speciation: a key point in the field of nuclear toxicology studies. J. Anal. At. Spectrom 26, 593. https://doi.org/10.1039/c0ja00223b.

Brown, J.E., Alfonso, B., Avila, R., Beresford, N.A., Copplestone, D., Pröhl, G., Ulanovsky, A., 2008. The ERICA tool. J. Environ. Radioact. 99, 1371–1383. https://doi.org/10.1016/j.jenvrad.2008.01.008.

Chandwadkar, P., Misra, H.S., Acharya, C., 2018. Uranium biomineralization induced by a metal tolerant *Serratia* strain under acid, alkaline and irradiated conditions. Metallomics 10, 1078–1088. https://doi.org/10.1039/C8MT00061A.

Choudhary, S., Sar, P., 2011. Uranium biomineralization by a metal resistant Pseudomonas aeruginosa strain isolated from contaminated mine waste. J. Hazard. Mater. 186, 336–343. https://doi.org/10.1016/j.jhazmat.2010.11.004.

Cumberland, S.A., Douglas, G., Grice, K., Moreau, J.W., 2016. Uranium mobility in organic matter-rich sediments: a review of geological and geochemical processes. Earth Sci. Rev. 159, 160–185. https://doi.org/10.1016/j.earscirev.2016.05.010.

Dang, D.H., Wang, W., Pelletier, P., Poulain, A.J., Evans, R.D., 2018. Uranium dispersion from U tailings and mechanisms leading to U accumulation in sediments: insights from biogeochemical and isotopic approaches. Sci. Total Environ. 610–611, 880–891. https://doi.org/10.1016/j.scitotenv.2017.08.156.

Ding, C., Cheng, W., Nie, X., 2019. Microorganisms and radionuclides. In: Interface Science and Technology. Elsevier, pp. 107–139. https://doi.org/10.1016/B978-0-08-102727-1.00003-0.

Duhamel, S., Jacquet, S., 2006. Flow cytometric analysis of bacteria- and virus-like particles in lake sediments. J. Microbiol. Methods 64, 316–332. https://doi.org/10.1016/j.mimet.2005.05.008.

Escudié, F., Auer, L., Bernard, M., Mariadassou, M., Cauquil, L., Vidal, K., Maman, S., Hernandez-Raquet, G., Combes, S., Pascal, G., 2018. FROGS: find, rapidly, OTUs with galaxy solution. Bioinformatics 34, 1287–1294. https://doi.org/10.1093/bioinformatics/btx791.

Fashola, M., Ngole-Jeme, V., Babalola, O., 2016. Heavy metal pollution from gold mines: environmental effects and bacterial strategies for resistance. IJERPH 13, 1047. https://doi.org/10.3390/ijerph13111047.

Gadd, G.M., 1986. The Uptake of Heavy Metals by fungi and Yeasts: The Chemistry and Physiology of the Process and Applications for Biotechnology. Immobilisation of Ions by Biosorption. Ellis Horwood, Chichester, UK, pp. 135–147.

Gadd, G.M., Fomina, M., 2011. Uranium and fungi. Geomicrobiol J. 28, 471–482. https://doi.org/10.1080/01490451.2010.508019.

Garland, J.L., Mills, A.L., 1991. Classification and characterization of heterotrophic microbial communities on the basis of patterns of community-level sole-carbon-source utilization. Appl. Environ. Microbiol. 57, 2351–2359. https://doi.org/10.1128/aem.57.8.2351-2359.1991.

Garland, J.L., Mills, A.L., Young, J.S., 2001. elative effectiveness of kinetic analysis vs single point readings for classifying environmental samples based on community-level physiological pro®les (CLPP). Soil Biol.

Giardine, B., Riemer, C., Hardison, R.C., Burhans, R., Elnitski, L., Shah, P., Zhang, Y., Blankenberg, D., Albert, I., Taylor, J., Miller, W., Kent, W.J., Nekrutenko, A., 2005. Galaxy: a platform for interactive large-scale genome analysis. Genome Res. 15, 1451–1455. https://doi.org/10.1101/gr.4086505.

Goberna, M., Insam, H., Klammer, S., Pascual, J.A., Sánchez, J., 2005. Microbial community structure at different depths in disturbed and undisturbed semiarid Mediterranean Forest soils. Microb. Ecol. 50, 315–326. https://doi.org/10.1007/s00248-005-0177-0.

Goecks, J., Nekrutenko, A., Taylor, J., Galaxy Team, T., 2010. Galaxy: a comprehensive approach for supporting accessible, reproducible, and transparent computational research in the life sciences. Genome Biol. 11, R86. https://doi.org/10.1186/gb-2010-11-8-r86.

Grangeon, S., Roux, C., Lerouge, C., Chardon, P., Beuzeval, R., Montavon, G., Claret, F., Grangeon, T., 2023. Geochemical and mineralogical characterization of streams and wetlands downstream a former uranium mine (Rophin, France). Appl. Geochem. 150, 105586 https://doi.org/10.1016/j.apgeochem.2023.105586.

Heidari, F., Riahi, H., Aghamiri, M.R., Zakeri, F., Shariatmadari, Z., Hauer, T., 2018. ^{226}Ra, ^{238}U and Cd adsorption kinetics and binding capacity of two cyanobacterial strains isolated from highly radioactive springs and optimal conditions for maximal removal effects in contaminated water. Int. J. Phytoremediation 20, 369–377. https://doi.org/10.1080/15226514.2017.1393392.

Hoyos-Hernandez, C., Courbert, C., Simonucci, C., David, S., Vogel, T.M., Larose, C., 2019. Community structure and functional genes in radionuclide contaminated soils in Chernobyl and Fukushima. FEMS Microbiol. Lett. 366, fnz180. https://doi.org/10.1093/femsle/fnz180.

Hui, N., Jumpponen, A., Niskanen, T., Liimatainen, K., Jones, K.L., Koivula, T., Romantschuk, M., Strömmer, R., 2011. EcM fungal community structure, but not diversity, altered in a Pb-contaminated shooting range in a boreal coniferous forest

site in southern Finland: ectomycorrhizal fungi and Pb contamination. FEMS Microbiol. Ecol. 76, 121–132. https://doi.org/10.1111/j.1574-6941.2010.01038.x.
Husson, A., Leermakers, M., Descostes, M., Lagneau, V., 2019. Environmental geochemistry and bioaccumulation/bioavailability of uranium in a post-mining context – the bois-noirs Limouzat mine (France). Chemosphere 236, 124341. https://doi.org/10.1016/j.chemosphere.2019.124341.
Ihrmark, K., Bödeker, I.T.M., Cruz-Martinez, K., Friberg, H., Kubartova, A., Schenck, J., Strid, Y., Stenlid, J., Brandström-Durling, M., Clemmensen, K.E., Lindahl, B.D., 2012. New primers to amplify the fungal ITS2 region - evaluation by 454-sequencing of artificial and natural communities. FEMS Microbiol. Ecol. 82, 666–677. https://doi.org/10.1111/j.1574-6941.2012.01437.x.
IRSN, 2018. IRSN MIMAUSA Database, Memory and Impact of Uranium Mines: Synthesis and Records. URL. https://mimausabdd.irsn.fr.
Islam, E., Sar, P., 2011. Molecular assessment on impact of uranium ore contamination in soil bacterial diversity. Int. Biodeter. Biodegr. 65, 1043–1051. https://doi.org/10.1016/j.ibiod.2011.08.005.
Jaswal, R., Pathak, A., Chauhan, A., 2019. Metagenomic evaluation of bacterial and fungal assemblages enriched within diffusion chambers and microbial traps containing uraniferous soils. Microorganisms 7, 324. https://doi.org/10.3390/microorganisms7090324.
Kazy, S.K., D'Souza, S.F., Sar, P., 2009. Uranium and thorium sequestration by a Pseudomonas sp.: mechanism and chemical characterization. J. Hazard. Mater. 163, 65–72. https://doi.org/10.1016/j.jhazmat.2008.06.076.
Kenarova, A., Radeva, G., Traykov, I., Boteva, S., 2014. Community level physiological profiles of bacterial communities inhabiting uranium mining impacted sites. Ecotoxicol. Environ. Saf. 100, 226–232. https://doi.org/10.1016/j.ecoenv.2013.11.012.
Khemiri, A., Carrière, M., Bremond, N., Ben Mlouka, M.A., Coquet, L., Llorens, I., Chapon, V., Jouenne, T., Cosette, P., Berthomieu, C., 2014. Escherichia coli response to uranyl exposure at low pH and associated protein regulations. PloS One 9, e89863. https://doi.org/10.1371/journal.pone.0089863.
Kolovi, S., Fois, G.-R., Lanouar, S., Chardon, P., Miallier, D., Baker, L.-A., Bailly, C., Beauger, A., Biron, D.G., David, K., Montavon, G., Pilleyre, T., Schoefs, B., Breton, V., Maigne, L., with the TIRAMISU Collaboration, 2023. Assessing radiation dosimetry for microorganisms in naturally radioactive mineral springs using GATE and Geant4-DNA Monte Carlo simulations. PloS One 18, e0292608. https://doi.org/10.1371/journal.pone.0292608.
Konietschke, F., Placzek, M., Schaarschmidt, F., Hothorn, L.A., 2015. Nparcomp: an *R* software package for nonparametric multiple comparisons and simultaneous confidence intervals. J. Stat. Soft. 64 https://doi.org/10.18637/jss.v064.i09.
Krawczyk-Bärsch, E., Gerber, U., Müller, K., Moll, H., Rossberg, A., Steudtner, R., Merroun, M.L., 2018. Multidisciplinary characterization of U(VI) sequestration by Acidovorax facilis for bioremediation purposes. J. Hazard. Mater. 347, 233–241. https://doi.org/10.1016/j.jhazmat.2017.12.030.
Kujala, K., Mikkonen, A., Saravesi, K., Ronkanen, A.-K., Tiirola, M., 2018. Microbial diversity along a gradient in peatlands treating mining-affected waters. FEMS Microbiol. Ecol. 94 https://doi.org/10.1093/femsec/fiy145.
Le, T.-H.-H., Michel, H., Champion, J., 2019. 210Po sequential extraction applied to wetland soils at uranium mining sites. J. Environ. Radioact. 199–200, 1–6. https://doi.org/10.1016/j.jenvrad.2018.12.027.
Li, B., Wu, W.-M., Watson, D.B., Cardenas, E., Chao, Y., Phillips, D.H., Mehlhorn, T., Lowe, K., Kelly, S.D., Li, P., Tao, H., Tiedje, J.M., Criddle, C.S., Zhang, T., 2018. Bacterial community shift and coexisting/Coexcluding patterns revealed by network analysis in a uranium-contaminated site after bioreduction followed by Reoxidation. Appl. Environ. Microbiol. 84 https://doi.org/10.1128/AEM.02885-17 e02885-17.
Ma, Y., Wang, Y., Chen, Q., Li, Y., Guo, D., Nie, X., Peng, X., 2020. Assessment of heavy metal pollution and the effect on bacterial community in acidic and neutral soils. Ecol. Indic. 117, 106626 https://doi.org/10.1016/j.ecolind.2020.106626.
Mahé, F., Rognes, T., Quince, C., de Vargas, C., Dunthorn, M., 2014. Swarm: robust and fast clustering method for amplicon-based studies. PeerJ 2, e593. https://doi.org/10.7717/peerj.593.
Manini, E., Danovaro, R., 2006. Synoptic determination of living/dead and active/dormant bacterial fractions in marine sediments: living/dead, active/dormant bacteria in marine sediments. FEMS Microbiol. Ecol. 55, 416–423. https://doi.org/10.1111/j.1574-6941.2005.00042.x.
Markich, S.J., 2002. Uranium speciation and bioavailability in aquatic systems: an overview. Scientific World Journal 2, 707–729. https://doi.org/10.1100/tsw.2002.130.
Martin, A., Hassan-Loni, Y., Fichtner, A., Péron, O., David, K., Chardon, P., Larrue, S., Gourgiotis, A., Sachs, S., Arnold, T., Grambow, B., Stumpf, T., Montavon, G., 2020. An integrated approach combining soil profile, records and tree ring analysis to identify the origin of environmental contamination in a former uranium mine (Rophin, France). Sci. Total Environ. 747, 141295 https://doi.org/10.1016/j.scitotenv.2020.141295.
Martin, A., Montavon, G., Landesman, C., 2021. A combined DGT-DET approach for an in situ investigation of uranium resupply from large soil profiles in a wetland impacted by former mining activities. Chemosphere 279, 130526. https://doi.org/10.1016/j.chemosphere.2021.130526.
Mehta, N., Benzerara, K., Kocar, B.D., Chapon, V., 2019. Sequestration of radionuclides Radium-226 and Strontium-90 by cyanobacteria forming intracellular calcium carbonates. Environ. Sci. Technol. 53, 12639–12647. https://doi.org/10.1021/acs.est.9b03982.
Merroun, M.L., Selenska-Pobell, S., 2008. Bacterial interactions with uranium: an environmental perspective. J. Contam. Hydrol. 102, 285–295. https://doi.org/10.1016/j.jconhyd.2008.09.019.
Merroun, M.L., Raff, J., Rossberg, A., Hennig, C., Reich, T., Selenska-Pobell, S., 2005. Complexation of uranium by cells and S-layer sheets of *Bacillus sphaericus* JG-A12. Appl. Environ. Microbiol. 71, 5532–5543. https://doi.org/10.1128/AEM.71.9.5532-5543.2005.
Merroun, M.L., Nedelkova, M., Ojeda, J.J., Reitz, T., Fernández, M.L., Arias, J.M., Romero-González, M., Selenska-Pobell, S., 2011. Bio-precipitation of uranium by two bacterial isolates recovered from extreme environments as estimated by potentiometric titration, TEM and X-ray absorption spectroscopic analyses. J. Hazard. Mater. 197, 1–10. https://doi.org/10.1016/j.jhazmat.2011.09.049.
Mikryukov, V.S., Dulya, O.V., Modorov, M.V., 2020. Phylogenetic signature of fungal response to long-term chemical pollution. Soil Biol. Biochem. 140, 107644 https://doi.org/10.1016/j.soilbio.2019.107644.
Momčilović, M., Kovačević, J., Tanić, M., Đorđević, M., Bačić, G., Dragović, S., 2013. Distribution of natural radionuclides in surface soils in the vicinity of abandoned uranium mines in Serbia. Environ. Monit. Assess. 185, 1319–1329. https://doi.org/10.1007/s10661-012-2634-9.
Mondani, L., Benzerara, K., Carrière, M., Christen, R., Mamindy-Pajany, Y., Février, L., Marmier, N., Achouak, W., Nardoux, P., Berthomieu, C., Chapon, V., 2011. Influence of uranium on bacterial communities: a comparison of natural uranium-rich soils with controls. PloS One 6, e25771. https://doi.org/10.1371/journal.pone.0025771.
Narendrula-Kotha, R., Nkongolo, K.K., 2017. Bacterial and fungal community structure and diversity in a mining region under long-term metal exposure revealed by metagenomics sequencing. Ecol. Genet. Genom. 2, 13–24. https://doi.org/10.1016/j.egg.2016.11.001.
Pan, X., Zhang, S., Zhong, Q., Gong, G., Wang, G., Guo, X., Xu, X., 2020. Effects of soil chemical properties and fractions of Pb, cd, and Zn on bacterial and fungal communities. Sci. Total Environ. 715, 136904 https://doi.org/10.1016/j.scitotenv.2020.136904.
Pennanen, T., Frostegard, A., Fritze, H., Baath, E., 1996. Phospholipid fatty acid composition and heavy metal tolerance of soil microbial communities along two heavy metal-polluted gradients in coniferous forests. Appl. Environ. Microbiol. 62, 420–428. https://doi.org/10.1128/aem.62.2.420-428.1996.
R Core Team, 2021. R: A Language and Environment for Statistical Computing. R Foundation for Statistical Computing, Vienna, Austria. URL.
Radeva, G., Kenarova, A., Bachvarova, V., Flemming, K., Popov, I., Vassilev, D., Selenska-Pobell, S., 2013. Bacterial diversity at abandoned uranium mining and milling sites in Bulgaria as revealed by 16S rRNA genetic diversity study. Water Air Soil Pollut. 224, 1748. https://doi.org/10.1007/s11270-013-1748-1.
Regvar, M., Likar, M., Piltaver, A., Kugonič, N., Smith, J.E., 2010. Fungal community structure under goat willows (Salix caprea L.) growing at metal polluted site: the potential of screening in a model phytostabilisation study. Plant and Soil 330, 345–356. https://doi.org/10.1007/s11104-009-0207-7.
Rogiers, T., Claesen, J., Van Gompel, A., Vanhoudt, N., Mysara, M., Williamson, A., Leys, N., Van Houdt, R., Boon, N., Mijnendonckx, K., 2021. Soil microbial community structure and functionality changes in response to long-term metal and radionuclide pollution. Environ. Microbiol. 23, 1670–1683. https://doi.org/10.1111/1462-2920.15394.
Rohart, F., Gautier, B., Singh, A., Lê Cao, K.-A., 2017. mixOmics: an R package for 'omics feature selection and multiple data integration. PLoS Comput. Biol. 13, e1005752 https://doi.org/10.1371/journal.pcbi.1005752.
Rosales-Castillo, J., Oyama, K., Vázquez-Garcidueñas, Ma, Aguilar-Romero, R., García-Oliva, F., Vázquez-Marrufo, G., 2017. Fungal community and ligninolytic enzyme activities in Quercus deserticola Trel. Litter from forest fragments with increasing levels of disturbance. Forests 9, 11. https://doi.org/10.3390/f9010011.
Salbu, B., 2007. Speciation of radionuclides – analytical challenges within environmental impact and risk assessments. J. Environ. Radioact. 96, 47–53. https://doi.org/10.1016/j.jenvrad.2007.01.028.
Sitte, J., Löffler, S., Burkhardt, E.-M., Goldfarb, K.C., Büchel, G., Hazen, T.C., Küsel, K., 2015. Metals other than uranium affected microbial community composition in a historical uranium-mining site. Environ. Sci. Pollut. Res. 22, 19326–19341. https://doi.org/10.1007/s11356-015-4791-1.
Stępniewska, H., Uzarowicz, Ł., Błońska, E., Kwasowski, W., Słodczyk, Z., Gałka, D., Hebda, A., 2020. Fungal abundance and diversity as influenced by properties of Technosols developed from mine wastes containing iron sulphides: a case study from abandoned iron sulphide and uranium mine in Rudki, south-central Poland. Appl. Soil Ecol. 145, 103349 https://doi.org/10.1016/j.apsoil.2019.08.011.
Stetten, L., Blanchart, P., Mangeret, A., Lefebvre, P., Le Pape, P., Brest, J., Merrot, P., Julien, A., Proux, O., Webb, S.M., Bargar, J.R., Cazala, C., Morin, G., 2018. Redox fluctuations and organic complexation govern uranium redistribution from U(IV)-phosphate minerals in a mining-polluted wetland soil, Brittany, France. Environ. Sci. Technol. 52, 13099–13109. https://doi.org/10.1021/acs.est.8b03031.
Suriya, J., Chandra Shekar, M., Nathani, N.M., Suganya, T., Bharathiraja, S., Krishnan, M., 2017. Assessment of bacterial community composition in response to uranium levels in sediment samples of sacred Cauvery River. Appl. Microbiol. Biotechnol. 101, 831–841. https://doi.org/10.1007/s00253-016-7945-2.
Sutcliffe, B., Chariton, A.A., Harford, A.J., Hose, G.C., Stephenson, S., Greenfield, P., Midgley, D.J., Paulsen, I.T., 2018. Insights from the genomes of microbes thriving in uranium-enriched sediments. Microb. Ecol. 75, 970–984. https://doi.org/10.1007/s00248-017-1102-z.
Sutcliffe, B., Hose, G.C., Harford, A.J., Midgley, D.J., Greenfield, P., Paulsen, I.T., Chariton, A.A., 2019. Microbial communities are sensitive indicators for freshwater sediment copper contamination. Environ. Pollut. 247, 1028–1038. https://doi.org/10.1016/j.envpol.2019.01.104.
Tedersoo, L., Bahram, M., Põlme, S., Kõljalg, U., Yorou, N.S., Wijesundera, R., Ruiz, L.V., Vasco-Palacios, A.M., Thu, P.Q., Suija, A., Smith, M.E., Sharp, C., Saluveer, E., Saitta, A., Rosas, M., Riit, T., Ratkowsky, D., Pritsch, K., Põldmaa, K.,

Piepenbring, M., Phosri, C., Peterson, M., Parts, K., Pärtel, K., Otsing, E., Nouhra, E., Njouonkou, A.L., Nilsson, R.H., Morgado, L.N., Mayor, J., May, T.W., Majuakim, L., Lodge, D.J., Lee, S.S., Larsson, K.-H., Kohout, P., Hosaka, K., Hiiesalu, I., Henkel, T. W., Harend, H., Guo, L., Greslebin, A., Grelet, G., Geml, J., Gates, G., Dunstan, W., Dunk, C., Drenkhan, R., Dearnaley, J., De Kesel, A., Dang, T., Chen, X., Buegger, F., Brearley, F.Q., Bonito, G., Anslan, S., Abell, S., Abarenkov, K., 2014. Global diversity and geography of soil fungi. Science 346, 1256688. https://doi.org/10.1126/science.1256688.

Ulanovsky, A., Pröhl, G., 2006. A practical method for assessment of dose conversion coefficients for aquatic biota. Radiat. Environ. Biophys. 45, 203–214. https://doi.org/10.1007/s00411-006-0061-4.

Violante, A., Cozzolino, V., Perelomov, L., Caporale, A.G., Pigna, M., 2010. Mobility and bioavailability of heavy metals and metalloids in soil environments. J. Soil Sci. Plant Nutr. 10 https://doi.org/10.4067/S0718-95162010000100005.

Wang, Y., Qian, P.-Y., 2009. Conservative fragments in bacterial 16S rRNA genes and primer design for 16S ribosomal DNA amplicons in metagenomic studies. PloS One 4, e7401. https://doi.org/10.1371/journal.pone.0007401.

White, T.J., Bruns, T., Lee, S., Taylor, J., 1990. Amplification and direct sequencing of fungal ribosomal rna genes for phylogenetics. In: PCR Protocols. Elsevier, pp. 315–322. https://doi.org/10.1016/B978-0-12-372180-8.50042-1.

Yan, X., Luo, X., 2015. Radionuclides distribution, properties, and microbial diversity of soils in uranium mill tailings from southeastern China. J. Environ. Radioact. 139, 85–90. https://doi.org/10.1016/j.jenvrad.2014.09.019.

Yin, K., Wang, Q., Lv, M., Chen, L., 2019. Microorganism remediation strategies towards heavy metals. Chem. Eng. J. 360, 1553–1563. https://doi.org/10.1016/j.cej.2018.10.226.

Zafar, S., Aqil, F., Ahmad, I., 2007. Metal tolerance and biosorption potential of filamentous fungi isolated from metal contaminated agricultural soil. Bioresour. Technol. 98, 2557–2561. https://doi.org/10.1016/j.biortech.2006.09.051.

Zeng, T., Mo, G., Hu, Q., Wang, G., Liao, W., Xie, S., 2020. Microbial characteristic and bacterial community assessment of sediment sludge upon uranium exposure. Environ. Pollut. 261, 114176 https://doi.org/10.1016/j.envpol.2020.114176.

Zhao, X., Huang, J., Lu, J., Sun, Y., 2019. Study on the influence of soil microbial community on the long-term heavy metal pollution of different land use types and depth layers in mine. Ecotoxicol. Environ. Saf. 170, 218–226. https://doi.org/10.1016/j.ecoenv.2018.11.136.